available at www.sciencedirect.com

ScienceDirect

journal homepage: www.ejconline.com

Identification of glia maturation factor beta as an independent prognostic predictor for serous ovarian cancer

Yan Li Li [a], Feng Ye [a], Xiao Dong Cheng [b], Ying Hu [a], Cai Yun Zhou [c], Wei Guo LÜ [a,b], Xing Xie [a,b,*]

[a] Women's Reproductive Health Laboratory of Zhejiang Province, Women's Hospital, School of Medicine, Zhejiang University, Hangzhou, China

[b] Department of Gynecologic Oncology, Women's Hospital, School of Medicine, Zhejiang University, Hangzhou, China

[c] Department of Pathology, Women's Hospital, School of Medicine, Zhejiang University, Hangzhou, China

ARTICLE INFO

Article history:
Received 27 January 2010
Received in revised form 6 April 2010
Accepted 19 April 2010
Available online 22 May 2010

Keywords:
Serous ovarian cancer
Glia maturation factor beta (GMFB)
Proteomics
Prognosis

ABSTRACT

Serous ovarian carcinoma (SOC) is the most common subtype of epithelial ovarian cancer which remains the leading cause of death from gynaecologic malignancy. Further knowledge of the proteins involved in serous ovarian cancer may lead to new treatment targets, new markers for early detection or prognosis prediction. In this study, we applied proteomic techniques to analyse the protein expression profiles of SOC and normal ovarian epithelium tissues. Totally 54 aberrantly expressed proteins were identified using 2-DE combined with MALDI-TOF/TOF. Six of these proteins were validated by western blot. Corresponding gene expression analysis of these proteins was also performed using real-time quantitative reverse transcription-polymerase chain reaction (RT-PCR). Additionally, we analysed glia maturation factor beta (GMFB) protein expression by immunohistochemistry in 246 patients with various degrees of ovarian epithelial lesions. GMFB expression in SOC was found to be significantly enhanced than that in normal epithelium, benign serous adenoma and borderline serous adenoma tissues, and was positively correlated with FIGO stage ($P = 0.012$). High GMFB expression was associated with poor disease-free survival ($P = 0.010$) and overall survival ($P = 0.003$), while multivariate analysis revealed GMFB to be an independent prognostic factor for disease-free survival ($P = 0.026$) and overall survival ($P = 0.006$) in patients with SOC. We therefore propose that proteins identified here may be involved in the development or progression of SOC, and GMFB can be considered as a prognostic predictor for SOC patients.

1. Introduction

Epithelial ovarian cancer is the leading course of death in women with gynaecological malignancy. About 205,000 cases of ovarian cancer are diagnosed worldwide each year.[1] Majority of the patients present extensive extraovarian spread at the time of diagnosis. The 5-year survival rate of advanced disease is only about 25%.[2] Although a large number of studies have demonstrated various molecules including genes and proteins associated with the development or progress of cancers, few of them are recognised to be specific for epithelial ovarian cancer. The finding of a new gene and its coding protein

* *Corresponding author:* Address: Women's Hospital, School of Medicine, Zhejiang University, Xueshi Rd. #2, Hangzhou 310006, China. Tel.: +86 571 87061501x1001; fax: +86 571 87061878.
E-mail address: xiex@mail.hz.zj.cn (X. Xie).

0959-8049/$ - see front matter
doi:10.1016/j.ejca.2010.04.015

associated with epithelial ovarian cancer will undoubtedly provide a novel potential target for diagnosis or treatment of the disease. Recently, differential gene expression analyses of ovarian cancer have been performed to identify candidate genes that may be involved in the development and progression of the disease.[3,4] However, it is well known that there is poor concordance between mRNA and protein expression.[5–7] Quantitative changes in protein expression but not gene expression can eventually reflect the phenotypic and biologic properties of ovarian cancer. Proteomics is a large-scale functional study on proteins. It has been expected to be a powerful tool to identify new diagnostic or predictive biomarkers, as well as promising therapeutic targets of cancers. However, only a few studies on proteome analysis of ovarian cancer have been reported up to date.

There are various subtypes of epithelial ovarian cancer. A recent study suggested that epithelial ovarian cancer is not a single disease. Depending on the histological subtypes, the same biomarker has different prognostic value and biomarker expression is constant from early to late stage, but only within a given subtype. The authors highlighted that ovarian cancer subtypes have distinct profiles, and better ways to detect and treat ovarian cancer are more likely to be found if future biomarker studies and clinical research studies investigate each subtype of ovarian carcinoma separately rather than grouping them all together.[8] Morphological heterogeneity of epithelial ovarian cancer has brought difficulties, interferences even biases for cancer research. Serous ovarian carcinoma (SOC) is the most common subtype of epithelial ovarian cancer that accounts for approximately 60–80% of all ovarian cancer cases and is by far the most aggressive histology. Thus, the study focusing on serous ovarian cancer will possess an important clinical significance.

Here we performed a proteome analysis of SOC instead of combining different subtypes of epithelial ovarian cancer together as some other studies did before.[9,10] The present study was aimed to investigate comparative protein expression in SOC versus normal ovarian epithelium and characterise tumour-specific changes in proteome of SOC. Our findings may bring out new potential diagnostic or prognostic predictor for SOC.

2. Materials and methods

2.1. Patients and sample preparation

Twenty SOC and 20 normal ovarian tissue specimens for protein and RNA extraction were immediately collected, dissected and snap-frozen in liquid nitrogen within about half an hour after resection from the patients, and finally stored at −80 °C for further use. All SOC samples comprised at least 85% tumour cells without necrosis. The normal ovarian tissues were confirmed to be free of any pathology.

Together with 45 normal ovarian epithelia, 51 benign ovarian serous adenomas and 40 borderline ovarian serous adenomas, a consecutive series of 110 formalin-fixed and paraffin-embedded specimens from patients diagnosed with SOC from April 25, 2000 to March 3, 2007 were obtained for immunohistochemical analysis. All cancer patients underwent cytoreductive surgery followed by taxol and platinum combination chemotherapy. Complete clinicopathologic data of the patients were collected and all the cancer patients were followed up by clinic interview or phone call. Of the 110 patients, 67 (60.9%) relapsed within the study period. A total of 52 patients died within the study period and 52 were alive at the last follow-up. Follow-up periods for survivors ranged from 8 to 107 months and the mean follow-up period was 48.39 months. Six patients were lost to follow-up.

All the specimens were obtained at the Women's Hospital, School of Medicine, Zhejiang University, China. All the histological diagnoses were reconfirmed by two pathologists and all cases of SOC were graded and staged according to the International Federation of Gynecology and Obstetrics (FIGO) standards. None of the patients were treated with chemotherapy, immunotherapy or radiotherapy prior to specimen collection. The normal ovarian tissue specimens were obtained from women who underwent bilateral adnexectomy because of benign gynaecological diseases. The study was approved by the Ethical Committee of Women's Hospital, School of Medicine, Zhejiang University.

2.2. Protein preparation

Total proteins were extracted from SOC and normal ovarian epithelium tissues. Approximately 300 mg of each specimen was homogenised and solubilised in 1000 μL of lysis buffer containing 7 M urea, 2 M thiourea, 4% w/v CHAPS, 1% w/v DTT, 2% v/v IPG buffer (Linear, pH 4–7, 24 cm, Bio-Rad), 1% v/v protease inhibitor cocktail and kept on ice for 1 h. After affixing 1% v/v protease inhibitor cocktail again, sonication was carried out on ice at a power of 75 W for 4 bursts of 8 s, each interspersed with 16 s. Then, the homogenate was centrifuged at 15,000*g* at 4 °C for 60 min.

The supernatant was used as the sample. Protein concentrations were determined using the Bradford protein assay (Bio-Rad).[11] At last, aliquots from the samples were stored at −80 °C.

2.3. Proteomics

2.3.1. Two-dimensional electrophoresis (2-DE)

A total of 350 μg protein samples were diluted to 450 μL with a rehydration solution containing 7 M urea, 2 M thiourea, 2% w/v CHAPS, 0.4% w/v DTT, 0.5% IPG buffer (pH 4–7) and 0.001% bromophenol blue and loaded on IPG strips (Liner, pH 4–7, 24 cm, Bio-Rad). Isoelectric focusing (IEF) was performed on a Protean IEF Cell (Bio-Rad, USA) according to the manufacturer's instruction. The total Vh achieved 100,000. Following IEF separation, strips were first incubated in the equilibration buffer (6 M urea, 50 mM Tris–HCl pH 8.8, 30% v/v glycerol, 2% SDS, 1% w/v DTT), and then alkylated in the same buffer containing 2.5% w/v iodoacetamide instead of DTT, each for 15 min. The second dimensional electrophoresis was carried out on 1.5 mm-thick 12% SDS–PAGE gels employing the Protean Plus Dodeca Cell at a constant power of 80 V and then 200 V till the bromophenol dye front reached the lower end of the gels. The electrophoresis unit was cooled at 20 °C with a water circulation system. Three representative 2-DE gels per sample were produced.

2.3.2. Gel staining and image analysis

The gels were subjected to modified silver staining method compatible with MS as previously described.[12] The stained gels were scanned using the high-resolution scanner GS-800 calibrated densitometer (Bio-Rad) followed by analysis with PDQUEST (v8.0.1, Bio-Rad) for spot detection, spot matching and spot quantification. The same parameters were used to detect spots in all of the gels in order to guarantee comparability between the gels. Reference gel was selected from one of the control gels and unmatched spots of the member gels were added to the reference gel by hand. The individual spot volume was normalised by the total quantity in valid spots on the gel to correct variations owing to silver staining and quantify protein spots. Quantitative analysis was carried out between the protein gels of both tumour and normal epithelium. Student's *t*-test statistical analysis with 99% significance level has been applied to the replicate groups. Significantly differentially expressed protein spots match the threshold ($\geqslant$2-fold) and statistical analysis standard was selected.

2.3.3. In-gel tryptic digestion

The differentially expressed protein spots were manually excised and subjected to in-gel tryptic digestion as previously described.[13]

2.3.4. MALDI-TOF/TOF MS and MS/MS analysis and database search

Peptide digest from each protein was mixed with 0.7 μL matrix solution (CHCA in ACN/water, 1:1, acidified with 0.1% TFA) and spotted onto a MALDI target plate at once, then allowed to air-dry. Mass analyses were performed on a 4700 MALDI-TOF/TOF Proteomics Analyzer (Applied Biosystems, USA) equipped with a 355-nm Nd:YAG laser. The instrument was operated in the positive ion reflection mode at 20 kV accelerating voltage and batch mode acquisition control. Parent mass peaks with mass range 700–3500 Da and minimum S/N 20 were picked out for tandem TOF/TOF analysis. The first five precursor ions with the highest intensity were selected for fragmentation. Two trypsin autolysis peaks at *m/z* 842.510 and 2211.105 were used to calibrate the instrument with internal calibration mode. 4700ExploreTM software (Applied Biosystems) was employed to process all acquired spectra of peptides in a default mode.Combined MS and MS/MS spectra were submitted to MASCOT (V2.1, Matrix Science, London, UK) by GPS Explore software (V3.6, Applied Biosystems, USA). The search parameters were as follows: ipi human 335 database, a maximum of one missed cleavage per peptide was allowed, a mass tolerance of 0.3 Da and MS/MS tolerance of 0.4 Da. Variable modifications such as carbamidomethylation for cysteine and oxidation for methionine were taken into account.MASCOT protein scores (based on combined MS and MS/MS spectra) higher than 64 were considered significant ($P < 0.05$). An ion score $\geqslant$95% confidence interval indicated that peptide fragmentation data were not randomly matched to the identified protein. Protein identification was further validated manually through BLAST using the SwissProt database.

2.4. Western blot

Western blot on six proteins of interest, Rho GDI 2, BANF1, Galectin-1, GGCT, glia maturation factor beta (GMFB) and HDGF, was performed on 20 SOC specimens (1 stage I, 5 stage II, 11 stage III and 2 stage IV) and 20 normal ovarian epithelium tissues. For detection of GGCT, Rho GDI 2 and HDGF, 25 μg protein was subjected to 12% SDS–PAGE and then transferred to 0.45 μm Immobilon-P transfer membranes (Millipore, USA) by electro-blotting. When measuring the expression of BANF1 and GMFB, 25 μg protein was separated by 15% SDS–PAGE and transferred onto 0.22 μm PVDF membranes (Millipore, USA). Membranes were blocked at RT for 1 h in TBST (50 mmol/l Tris–HCl, pH 7.6, 150 mmol/l Nacl, 0.1% Tween 20) containing 5% non-fat dry milk and then incubated with rabbit anti-BANF1 polyclone antibody (Abcam, 1:200 dilution), rabbit anti-GMFB polyclone antibody (proteintech Group, Inc., 1:1000 dilution), sheep anti-GGCT polyclone antibody (R&D system, 1:1000 dilution), rabbit anti-Rho GDI 2 polyclone antibody (abcam, 1:800 dilution), rabbit anti-HDGF polyclone antibody (Proteintech Group, Inc., 1:800 dilution), rabbit anti-galectin-1 polyclone antibody (abcam, 1:1000 dilution) and mouse anti-β-actin monoclone antibody (sigma, 1:3000 dilution) at 4 °C overnight. The membranes were then incubated with appropriate secondary antibody for 1 h at RT and visualised with an electrochemiluminescence detection system (Santa Cruz Biotechnology).

2.5. RNA isolation and real-time RT-PCR

Real-time quantitative reverse transcription-polymerase chain reaction (RT-PCR) was also performed on 20 frozen SOC specimens (1 stage I, 5 stage II, 11 stage III, and 2 stage IV) and 20 normal counterparts, the same cases used in western blot analysis. Total RNA was extracted using TRIzol reagent (Takara Biotechnology, Japan) following the manufacturer's instructions. After digesting with DNase I, the total RNA (20 μg) was subjected to reverse transcription using RT reagent (Takara Biotechnology, Japan). Intron spanning primer sets (Supplementary Table S1) specific for six genes corresponding with the six validated proteins were used. *ACTB* was selected for normalisation. SYBR green real-time RT-PCR was performed with an Applied Biosystems 7900HT Fast Real-time PCR system using the SYBR® Premix Ex Taq™ (perfect real-time) (TaKaRa Biotechnology, Japan) according to the manufacture's protocols. All reactions were run in triplicate. No template control reactions were included in each assay run and a melting curve was constructed for each primer pair to confirm product specificity. The expression levels of the six genes were calculated according to the $2^{-\Delta Ct}$ method. Average *Ct* value of each target gene was subtracted from the mean *Ct* value of *ACTB* to obtain a ΔCt value.

2.6. Immunohistochemistry

When using the selected anti-GMFB antibody in western blot analysis, a unique band was obtained, and therefore the same antibody was used in immunohistochemical analysis. Paraffin blocks were sliced at 5-mm intervals. The sections were deparaffinised in xylene and rehydrated using ethanol. Then,

hydrated autoclave pretreatment was performed by boiling the samples in 10 mM citrate buffer (pH 6.0) for 2 min. Endogen peroxidase was quenched with 3% hydrogen peroxidase for 10 min at room temperature. The slides were then incubated with the anti-GMFB antibody at a dilution of 1:500 in Tris-buffered solution (50 mM Tris–HCl, 150 mM NaCl, pH 7.4) at RT for 1 h followed by incubation with Dako Envision™ Peroxidase (Dako Diagnostica, Hamburg, Germany) for 30 min at RT. The antibody staining was visualised with 3,3-diaminobenzidine tetrahydrochloride (Dako, Dako Diagnostica, Hamburg, Germany). The section slides were counter-stained with Mayer's haematoxylin, dehydrated and mounted. Negative controls without incubation with primary antibody were processed. Stained sections were evaluated in a blind manner without prior knowledge of the clinicopathologic parameters by two independent observers and the average score for each slide were used for statistical analysis.

GMFB expression was evaluated as previously described.[14–16] The percentage of GMFB positive cells was semi-quantitatively determined by assessing the entire area of epithelia cells in each section. Each sample was assigned to one of the following categories: 0 (0–4%), 1 (5–24%), 2 (25–49%), 3 (50–74%) or 4 (75–100%). The intensity of immunostaining was graded as follows: 0, negative; 1+, weak; 2+, moderate or 3+, strong. A final score between 0 and 12 was obtained by multiplying the 2 scores. Scores of 9–12 were defined as 'high expression', scores of 5–8 were defined as 'moderate expression' and scores of 0–4 were defined as 'low expression'.

2.7. Statistics

Statistical analyses were performed using the SPSS 15.0 statistical software package. The data of western blot and real-time RT-PCR were assessed by student-*t* tests. The Kruskal–Wallis H and the Mann–Whitney U tests were used to evaluate the differences in GMFB expression among the different groups. Correlations between GMFB expression and the clinicopathologic parameters were evaluated by χ^2 test and Fisher's exact probability test. Overall survival was defined as time from first day after surgery to death or the last follow-up date. Disease-free survival was defined as time from first day after surgery to the first of either death or disease progression (assessed by CA125 increase and/or imaging examination). Survival curves were plotted by use of the Kaplan–Meier method and the difference in survival was compared by the log-rank test. The influence of various clinicopathologic features on survival was assessed by the Cox's proportional hazard model. $P < 0.05$ was considered statistically significant.

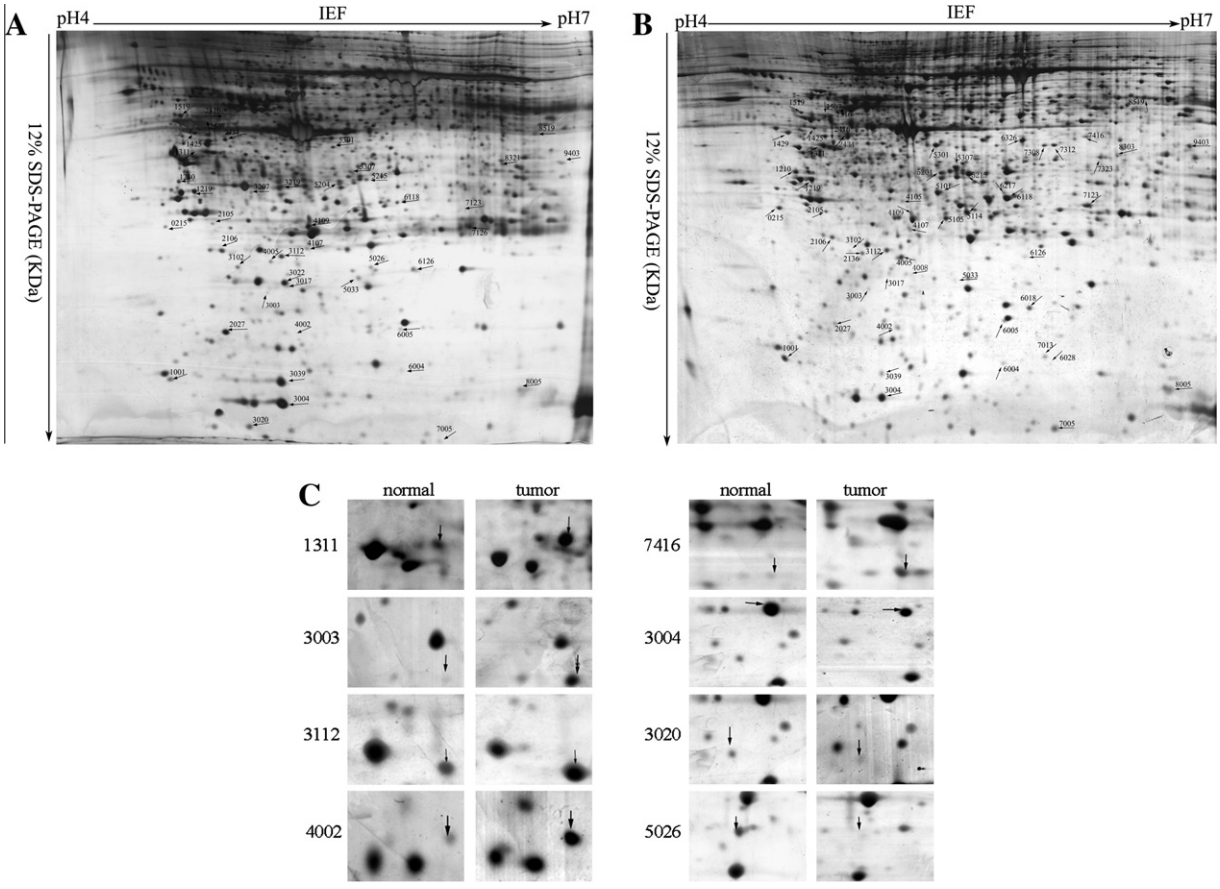

Fig. 1 – Identification of differentially expressed proteins in SOC. (A) Representative two-dimensional image of proteins detected in normal ovarian epithelium tissues. (B) Representative two-dimensional image of proteins detected in SOC tissues. Differentially expressed protein spots are marked with master numbers and arrows. (C) Zoomed maps of representative spots with differential expression.

Table 1 – Summary of proteins differentially expressed between the normal ovarian epithelium and SOC groups.

Spot ID[a]	Spot name	Gene symbol	Accession no.	Calculated Mr/pI (Da)	Protein score[b]	Confidence interval (%)	Sequence covered (%)[c]	Fold change (T/N)[d]	Main molecular function
Up regulated proteins									
0215	Eukaryotic translation initiation factor 6	EIF6	IPI00010105	26582.2/4.56	373	100	33.5	2.98	Mature ribosome assembly and translation
1001	ATP synthase delta chain, mitochondrial precursor	ATP5D	IPI00024920	17479.2/5.38	138	100	11.9	2.72	ATP synthesis and catabolism
1210	Proliferating cell nuclear antigen	PCNA	IPI00021700	28750.3/4.57	320	100	36.0	2.89	DNA repair, cell proliferation and signal transduction
1219	Isoform 2 of tropomyosin alpha-3 chain	TPM3	IPI00218319	29014.7/4.75	327	100	53.2	2.36	Cell motion, muscle contraction regulation
1311	Heptoma-derived growth factor	HDGF	IPI00020956	26771.9/4.7	267	100	47.5	2.86	Cell proliferation, involved in signal transduction
1429	Vitronectin precursor	VTN	IPI00298971	54271.2/5.55	151	100	10.3	3.79	Cell adhesion, cell-matrix adhesion and immune response
2105	Ubiquitin carboxyl-terminal hydrolase isozyme L3	UCHL3	IPI00514154	28199.2/6.39	219	100	28.7	2.19	Ubiquitin-dependent protein catabolism
2106	Isoform 1 of heat shock protein HSP 90-alpha	HSP90AA1	IPI00784295	84606.7/4.94	279	100	10.2	22.80	Protein complex assembly, protein folding, signal transduction, mitochondrial transport
2136	Set translocation	SET	IPI00646059	31114.3/4.09	87	99.986	13.0	∞	DNA replication, nucleosome assembly
2416	Keratin 8	KRT8	IPI00554648	53671.1/5.52	270	100	49.5	5.34	Contributes to apoptosis, cytoskeleton organisation as well as signal transduction
2434	Keratin 8	KRT8	IPI00554648	53671.1/5.52	700	100	50.9	8.63	Contributes to apoptosis, cytoskeleton organisation as well as signal transduction
3003	Isoform 1 of gamma-glutamylcyclotransferase	GGCT	IPI00031564	20994.3/5.07	284	100	45.2	13.01	Gamma-glutamylcyclotransferase activity
3017	Gamma actin	ACTG1	IPI00021440	41765.8/5.31	80	99.936	19.2	2.99	Cytoskeletal structural protein
3102	Heat shock protein HSP 90-beta	HSP90AB1	IPI00414676	83212.1/4.97	421	100	15.2	7.26	Stress response, ATP binding and protein folding
3112	Rho GDP-dissociation inhibitor 2	ARHGDIB	IPI00003817	22973.6/5.1	251	100	34.3	2.30	Rho protein signal transduction, immune response and negative regulation of cell adhesion
3207	Coatomer subunit epsilon	COPE	IPI00465132	34460.3/4.97	318	100	42.2	2.40	Protein transport and ER-golgi transport
4002	Glia maturation factor beta	GMFB	IPI00412987	18098.1/5.21	240	100	32.5	4.17	Growth factor
4005	Cathepsin B precursor	CTSB	IPI00295741	37796.8/5.88	136	100	14.7	6.77	Proteolysis, apoptosis regulation

4008	Chromobox protein homologue 3	CBX3	IPI00297579	20798.3/5.23	86	99.983	14.2	13.98	Transcription and transcription regulation
4105	Proteasome subunit alpha type 3	PSMA3	IPI00171199	27629.7/5.19	161	100	39.5	2.48	Protein catabolism
4107	Ubiquitin-conjugating enzyme E2K	HIP2	IPI00021370	22392.6/5.33	109	100	38.0	2.74	Protein modification and protein metabolism
5007	Cellular retinoic acid binding protein 2	CRABP2	IPI00643056	9245.8/5.43	98	99.999	13.0	24.96	Transport
5101	Proteasome activator subunit 2	PSME2	IPI00746205	27384.3/5.54	92	99.996	13.4	2.27	Regulation of ubiquitin-protein ligase activity
5204	Tubulin beta 2B	TUBB2B	IPI00031370	49920.9/4.78	116	100	43.4	2.01	GTP binding
5215	Inorganic pyrophosphates	PPA1	IPI00015018	32639.2/5.54	374	100	47.8	2.19	Phosphate metabolic process
5301	Stomatin-like protein 2	STOML2	IPI00334190	38510.2/6.88	405	100	46.9	2.34	Receptor binding
5307	Tubulin, alpha 1c	TUBA1C	IPI00478908	28545.4/5.24	415	100	54.9	3.31	GTP and protein binding
6004	Protein mago nashi homologue	MAGOH	IPI00219306	17152.8/5.74	291	100	61.6	2.56	RNA and protein binding
6005	Stathmin/oncoprotein 18	STMN1	IPI00642012	9858.3/6.75	291	100	24.2	3.09	Cell differentiation, signal transduction and microtubule depolymerisation
6018	Non-metastatic cells 1, Protein	NM23A	IPI00375531	19640.9/5.42	404	100	58.8	3.07	Negative regulation of cell cycle and cell proliferation, regulation of apoptosis and nucleotide metabolic process
6028	Protein mago nashi homologue	MAGOH	IPI00219306	17152.8/5.74	135	100	38.4	2.40	RNA and protein binding
6118	Proteasome activator complex subunit 1	PSME1	IPI00030154	28705/5.78	325	100	43.6	2.37	Protasome activator activity
6217	Proteasome activator Complex subunit 3	PSME3	IPI00030243	29487.6/5.69	334	100	51.2	3.12	Proteasome activator activity
6326	Alpha-enolase	ENO1	IPI00465248	47139.3/7.01	275	100	42.9	4.62	Glycolysis, negative regulation of cell growth and transcription
7005	S100 calcium-binding protein	S100A11	IPI00013895	11732.8/6.56	178	100	46.7	3.17	Negative regulation of DNA replication and cell proliferation
7013	Ubiquitin-conjugating enzyme E2N	UBE2N	IPI00003949	17127/6.13	393	100	49.3	2.22	Signal transduction, protein metabolism and DNA repair
7123	Endoplasmic reticulum protein ERP29 precursor	ERP29	IPI00024911	28975.2/6.77	93	99.997	19.2	3.34	Protein folding, secretion and transport
7308	Gelsolin-like capping protein	CAPG	IPI00848090	38474.5/5.82	269	100	30.7	4.48	Actin binding, protein complex assembly
7312	Macrophage-capping protein	CAPG	IPI00027341	38493.5/5.88	256	100	37.1	2.88	Actin binding, protein complex assembly
7416	DnaJ homologue subfamily B member 11	DNAJB11	IPI00008454	40488.6/5.81	439	100	52.8	2.78	Hear shock protein binding, protein folding an mRNA modification
8005	Stathmin/oncoprotein 18	STMN1	IPI00642012	9858.3/6.75	249	100	18.8	3.04	Cell differentiation, signal transduction and microtubule depolymerisation
9403	Sialic acid synthase	NANS	IPI00147874	40281.4/6.29	75	99.784	26.5	2.04	Carbohydrate and lipopolysaccharide biosynthetic

(*continued on next page*)

Table 1 – *continued*

Spot ID[a]	Spot name	Gene symbol	Accession no.	Calculated Mr/pI (Da)	Protein score[b]	Confidence interval (%)	Sequence covered (%)[c]	Fold change (T/N)[d]	Main molecular function
Down regulated proteins									
1425	Vimentin	VIM	IPI00827679	49623.1/5.19	588	100	50.2	0.34	Involved in intermediate filament-based process and cell motion
2027	Myosin regulatory light chain 2, smooth muscle isoform	MYL9	IPI00220278	19814.4/4.8	284	100	62.8	0.14	Regulation of muscle contraction
2507	Vimentin	VIM	IPI00827679	49623.1/5.19	526	100	51.3	0.31	Involved in intermediate filament-based process and cell motion
2516	Vimentin	VIM	IPI00827679	49623.1/5.19	577	100	50.0	0.36	Involved in intermediate filament-based process and cell motion
3004	Galectin-1	LGALS1	IPI00219219	14706.2/5.34	137	100	35.6	0.38	Involved in cell differentiation, regulation of apoptosis, and signal transduction
3039	Retinol-binding protein 1,cellular	RBP1	IPI00219718	22296.1/5.76	405	100	44.2	0.19	Retinol and retinoic acid metabolism, transport
3020	Barrier to autointegration factor 1	BANF1	IPI00026087	10052/5.81	251	100	55.1	0.23	Provirus integration
3219	Osteoglycin	OGN	IPI00025465	33900.9/5.46	229	100	22.5	0.38	Growth factor
3022	Isoform 1 of polymerase 1 and transcript release factor	PTRF	IPI00176903	43449.8/5.51	133	100	7.4	0.21	Transcription regulation
4109	Brain type mu-glutathione S-transferase	GSTM3	IPI00246975	26542.1/5.37	328	100	54.2	0.22	Glutathione transferase activity
5026	Glutathione peroxidase 3 Precursor	GPX3	IPI00026199	25489/8.2	150	100	23.5	0.22	Protects cells and enzymes from oxidative damage
5033	Haem-binding protein 1	HEBP1	IPI00148063	21083.5/5.71	325	100	70.4	0.29	Haem binding
5105	Ubiquitin carboxyl-terminal esterase L1	UCHL1	IPI00018352	24808.5/5.33	140	100	31.8	0.48	Ubiquitin-dependent protein catabolic process
5114	Serum amyloid P-component precursor	APCS	IPI00022391	25371.1/6.1	332	100	30.0	0.23	Acute-phase response, chaperone-mediated protein complex assembly and protein folding
6126	DJ-1	PARK7	IPI00298547	19878.5/6.33	282	100	47.6	0.43	Ras protein signal transduction and stress response
7126	Glutathione S-transferase Mu 2	GSTM2	IPI00219067	25728/6	271	100	64.7		Glutathione transferase activity
8321	Delta-aminolevulinic acid dehydratase	ALAD	IPI00010314	36271.4/6.32	125	100	18.9	0.39	Porphobilinogen synthase activity
8519	Retinal dehydrogenase 1	ALDH1A1	IPI00218914	54826.9/6.3	197	100	13.8	0.43	Cellular aldehyde metabolism and oxidation reduction

[a] Spot ID is the unique SSP number, which refers to the labels in Fig. 1.
[b] A score of more than 64 was significant ($P < 0.05$).
[c] The number of amino acids spanned by the assigned peptides divided by the sequence length.
[d] The fold change between SOC and normal ovarian epithelia.

3. Results

3.1. 2D and MALDI-TOF/TOF MS

Comparative 2D analysis of SOC ($n = 10$, 4 stage II, 6 stage III) and normal ovarian epithelium samples ($n = 10$) were performed to investigate the factors that might be related to SOC onset and progression. Approximately 1800 proteins spots were detected in both groups (Fig. 1A and B). Compared with the normal control group, 63 protein spots exhibited significantly differential expression, including 38 upregulated spots and 25 downregulated spots. Magnified comparison patterns of some representative protein spots are displayed in Fig. 1C.

Among the above-mentioned 63 spots, 60 were successfully identified by MALDI-TOF/TOF MS, representing 54 unambiguous and unique proteins (Table 1). GMFB and galectin-1 were selected as examples here. The mass spectra of the tryptic digests of GMFB and galectin-1 were presented in Fig. 2A and B, which was further confirmed by MS/MS analysis of peptides from each protein selected for fragmentation (Fig. 2C and D). The MASCOT MS/MS ion search information of all identified proteins are shown in Supplementary Table S2. According to the knowledge from Swiss-Prot/TrEMBL and Gene Ontology Database, these dysregulated proteins were classified in functional categories (Fig. 3). These proteins are mainly involved in metabolism or binding. In addition, a considerable number of proteins related to cell proliferation, differentiation and apoptosis were identified such as galectin-1, HDGF and PCNA.

3.2. Validation of differentially expressed proteins by western blot

To further confirm the protein alterations in SOC revealed by proteomic analysis, BANF1, galectin-1, GMFB, GGCT, HDGF and Rho GDI 2 were selected for validation. As shown in Fig. 4A and B, GMFB, GGCT, HDGF and Rho GDI 2 expression were upregulated in SOC compared with normal ovarian epithelium. Contrarily, BANF1 and galectin-1 expression were downregulated in SOC. The expression changes of these selected proteins were consistent with the 2-DE and silver-staining results.

3.3. Quantisation of corresponding gene expression level of selected proteins by real-time RT-PCR

To compare protein expression with their corresponding mRNA expression, the six genes, *GMFB*, *ARHGDIB*, *HDGF*, *GGCT*, *BANF1* and *LAGLS1*, were examined by real-time RT-PCR. As shown in Fig. 4C, the levels of *ARHGDIB* and *HDGF* mRNA expression were upregulated and those of *BANF1* and *LAGLS1* mRNA were downregulated in SOC compared with normal epithelium. But no changes of *GMFB* and *GGCT* mRNA expression were found in OSEC compared with its normal counterpart, which was not consistent with the alterations of protein expression.

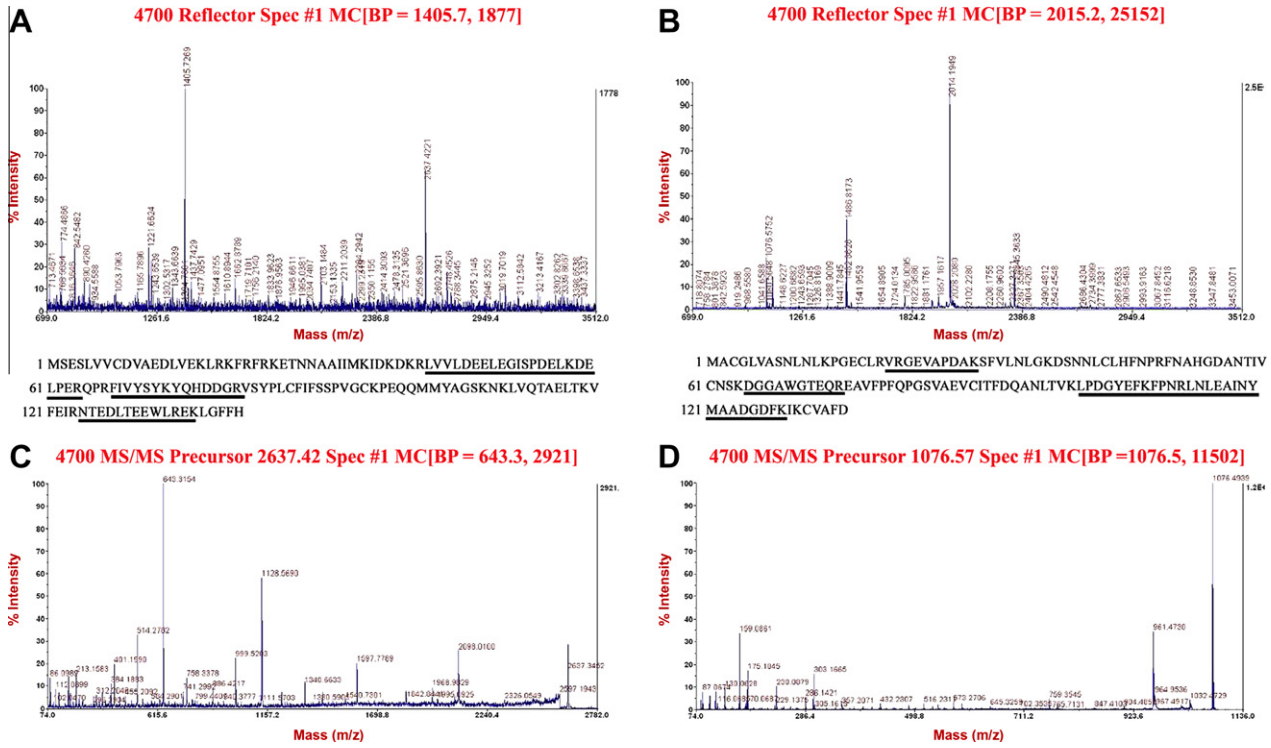

Fig. 2 – Identification of GMFB and galectin-1 by MALDI TOF-MS/MS. (A) MS spectrum with tryptic peptides of GMFB. The amino acid sequences with matched peptide sequences were underlined. (B) MS spectrum with tryptic peptides of galectin-1. The amino acid sequences with matched peptide sequences were underlined. (C) MS/MS spectrum of the peptide *m/z* 2637.42, in which the tryptic peptide sequences were confirmed from the labelled b- and y-ions. The sequence of precursor at *m/z* 2637.42 was analysed by MS/MS to be LVVLDEELEGISPDELKDELPER. (D) MS/MS spectrum of the peptide *m/z* 1076.57, which was confirmed to be DGGAWGTEQR.

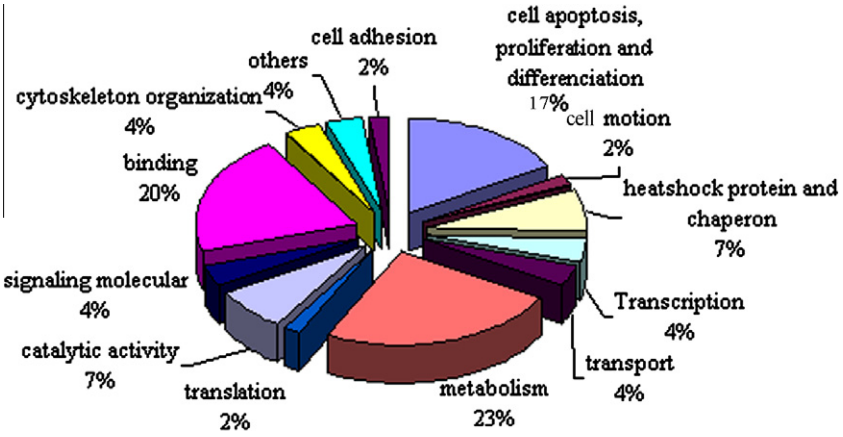

Fig. 3 – Functional categorisation of differentially expressed proteins between normal ovarian epithelium and SOC based on GO consortium.

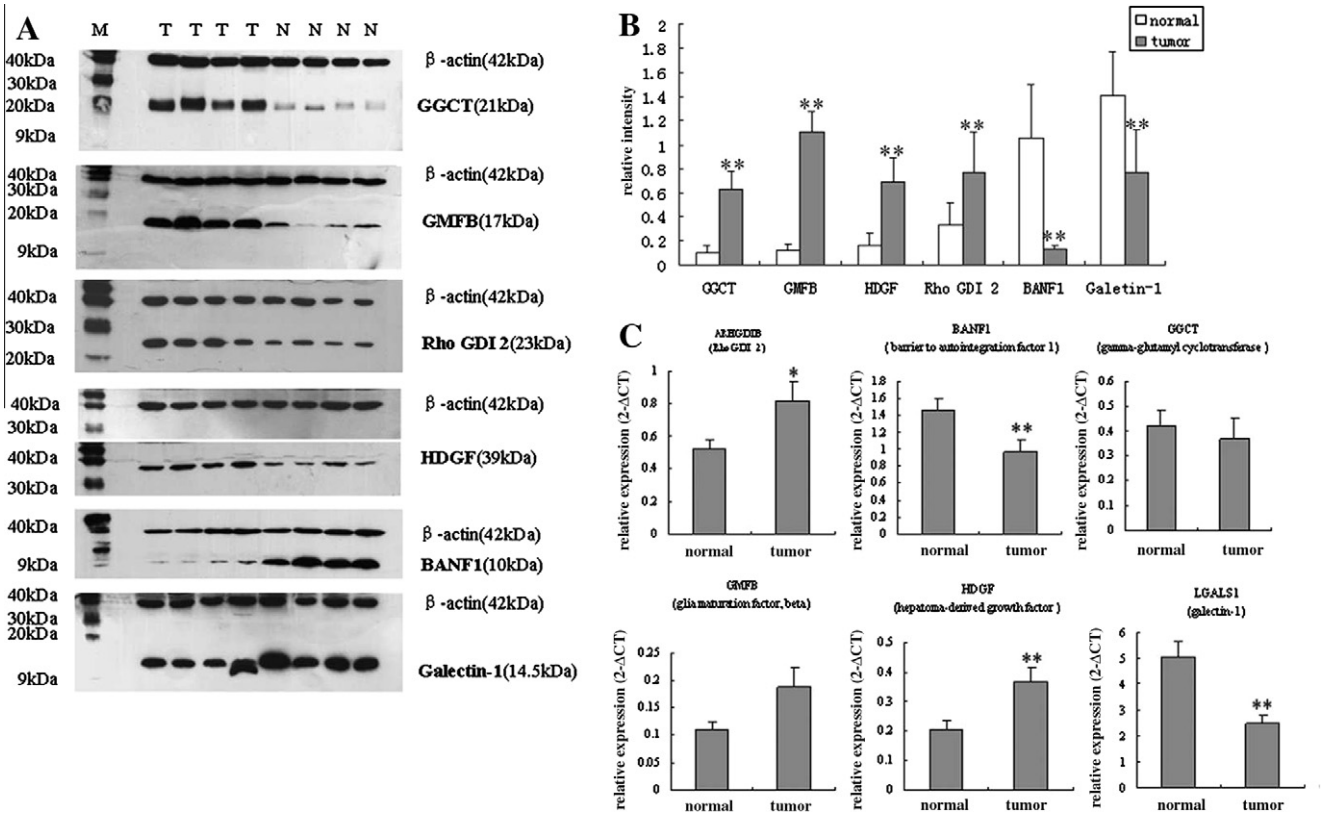

Fig. 4 – Western blot and real-time RT-PCR analyses of six proteins of interest. (A) The representative autoradiographs of GGCT, GMFB, HDGF, Rho GDI 2, BANF1 and Galectin-1. β-Actin signals were used for data normalisation. M, molecular marker; N, normal ovarian epithelium tissues; T, SOC tissues. (B) Densitometric quantification of protein levels in normal and tumour groups. Significantly different expressions were labelled with asterisks. (C) Real-time RT-PCR validation of mRNA expression level of *ARHGDI*, *BANF1*, *GGCT*, *GMFB*, *HDGF*, and *LGALS1*. The expression of *ACTB* was applied to normalise data. Significantly different expressions between normal ovarian epithelia and SOC were labelled with asterisks ($^{*}P < 0.05$, $^{**}P < 0.01$).

3.4. *Immunohistochemical analysis of GMFB*

3.4.1. *GMFB expression in various serous ovarian epithelial lesions*

Diverse intensities of immunoreactivity to GMFB staining were observed in the cytoplasm and nucleus of epithelium cells and significant difference was observed among the four groups ($\chi^2 = 73.964$, $P < 0.001$, Fig. 5A). In more detail, low GMFB expression was observed in 28 (62.2%) of 40 normal epithelia, 16 (31.4%) of 51 benign adenomas, 6 (15%) of 40 borderline adenomas and 10 (9.1%) of 110 SOCs. Moderate GMFB expression was detected in 14 (31.1%) normal epithelia, 28 (54.9%) benign adenomas, 17 (42.5%) borderline adenomas and 30 (27.3%) SOCs. Three (6.7%) epithelia, 7 (13.7%) benign

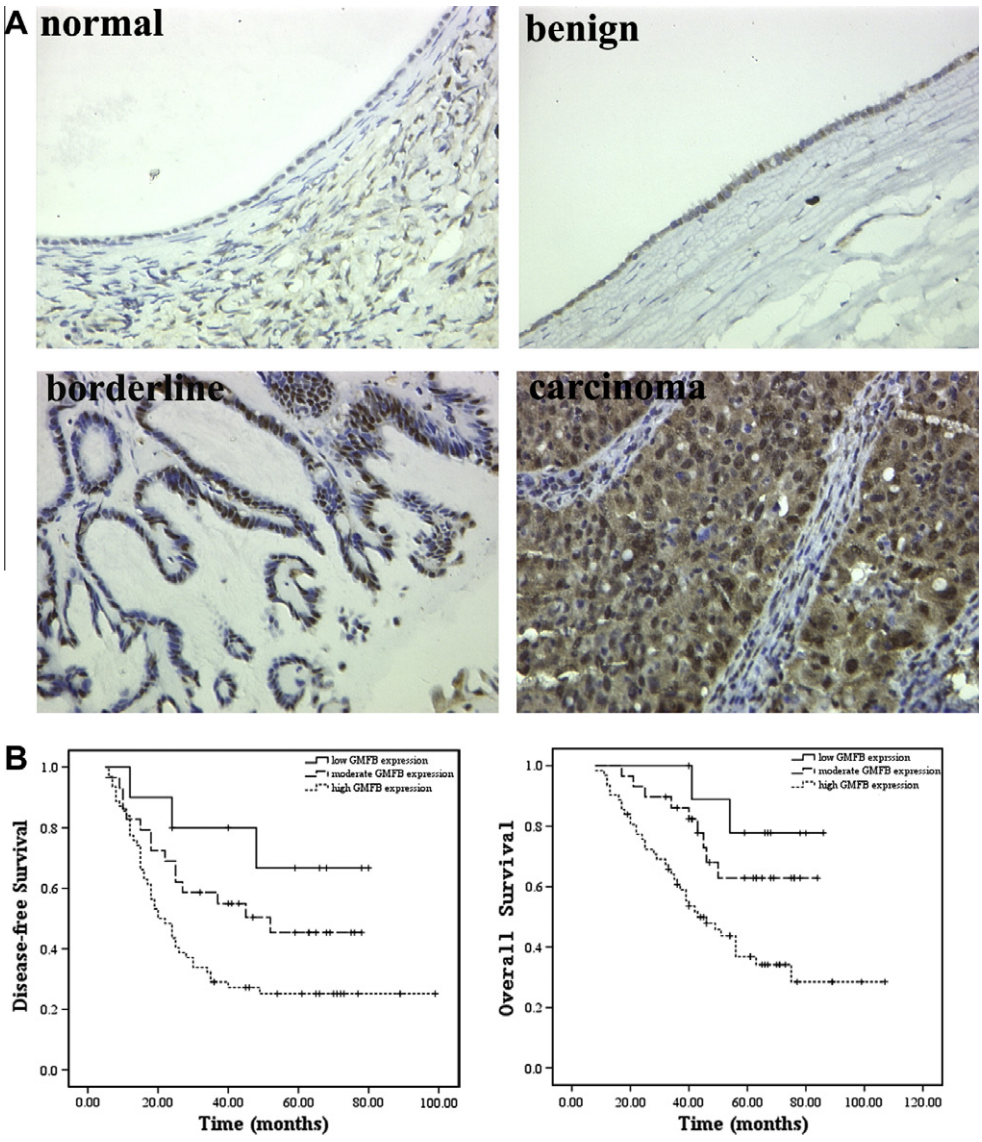

Fig. 5 – Immunohistochemistry and survival analysis of GMFB expression. (A) Staining of GMFB in normal ovarian epithelium, benign adenoma, borderline adenoma and carcinoma. The positive staining was both cytoplasmic and, more strongly, nuclear. (B) Kaplan–Meier curve for disease-free and overall survival in SOC patients with different GMFB expression degrees.

adenomas, 17 (42.5%) borderline adenomas and 70 (63.6%) SOCs showed high GMFB expression. The expression of GMFB in SOC was significantly enhanced than that in normal epithelial ($Z = -7.490$, $P < 0.001$), benign adenomas ($Z = -5.948$, $P < 0.001$) and borderline adenomas ($Z = -2.272$, $P = 0.023$).

3.4.2. *Correlation between GMFB expression and clinicopathologic features in SOC*

The correlation between GMFB expression and clinicopathological parameters in SOC was analysed (Table 2). GMFB expression was significantly correlated with FIGO stage ($P = 0.012$) of SOC patients, but no correlation was found between the GMFB expression and patient age, tumour grade, clinical response to chemotherapy, performance status, pretreatment serum CA125 level, ascitic fluid volume and residual disease.

3.4.3. *Survival analysis*

To investigate the prognostic value of GMFB expression, the association of GMFB expression with disease-free and overall survival in SOC patients was evaluated using Kaplan–Meier survival curves with the log-rank test and confirmed by univariate and multivariate Cox regression models. The 5-year disease-free survival rates of patients with high, moderate and low GMFB expression were 25.1%, 45.3% and 66.7%, while the overall 5-year survival rates were 36.8%, 62.8% and 77.8%, respectively. The patients with high level of GMFB protein expression exhibited significantly poorer disease-free ($P = 0.010$) and overall survival ($P = 0.003$) than patients with low and moderate GMFB expression groups (Fig. 5B). Since there were only 10 cases in low GMFB expression group and 70(63.6%) cases in high expression group, we gathered low and moderate groups together for Cox's proportional hazard

Table 2 – The relationship between GMFB expression and clinicopathologic features.

Variable	*n*	GMFB expression class			*P*-value
		Low	Moderate	High	
Age (years)					0.697
1: ⩽50	52	6	14	32	
2: >50	58	4	16	38	
FIGO stage					0.012**
1: I	7	2	4	1	
2: II	16	1	8	7	
3: III	79	7	17	55	
4: IV	8	0	1	7	
Tumour grade					0.987
1: G1 + G2	32	3	9	20	
2: G3	78	7	21	50	
Clinical response to chemotherapy					0.309
2: PR + CR	68	8	20	40	
1: All others 42	2	10	30		
Performance status					0.527
1: No impairment 75	7	18	50		
2: All others 35	3	12	20		
Pretreatment Serum CA125 (U/ml)					0.977
1: ⩽500	46	4	13	29	
2: >500	68	6	17	41	
Ascitic fluid volume (ml)					0.800
1: ⩽100	35	4	10	21	
2: >100	71	6	20	49	
Residual disease (cm)					0.665
1: ⩽2	71	7	21	43	
2: >2	39	3	9	27	

Abbreviations: PR, partial remission; CR, complete remission.
** Significant at the 0.01 level.

model analysis.[17] Univariate analysis revealed that GMFB expression, FIGO stage, clinical response to chemotherapy, ascitic fluid volume and residual disease predicted both disease-free and overall survival in this cohort. Further multivariate analysis showed that GMFB expression was an independent prognostic factor for both disease-free and overall survival of SOC patients after surgery, as well as FIGO stage and clinical response to chemotherapy (Table 3).

4. Discussion

Proteomic studies on epithelial ovarian cancer have been reported recently, but most of them used cultured cell lines as study objectives.[18–20] Thus, one cannot exclude the possibility that cultured tumour cells only represent a subpopulation of cancer cells that are derived from original tumour, or *in vitro* expansion conditions may have modified gene expression.[21,22] To avoid these disadvantages, others extracted proteins from surgical specimens for proteome analysis. However, they used grouping several subtypes of ovarian cancer together.[9,10] Recently, Li and colleagues[23] attempted to identify tumour-associated proteins in serous ovarian cystadenocarcinoma by comparing protein expression profile of cystadenocarcinoma versus normal epithelium. Consequently, they obtained only six differentially expressed proteins. It is likely that the use of short IPG strip (13 cm) with wide pH extent probably interfered protein separation and limited the display of aberrantly expressed protein spots.

In the present study, we focused only on SOC, avoiding interference spelled by pooling different pathohistologic subtypes. Then, we prepared proteins directly from SOC and normal ovarian epithelium tissues, which may better represent the status *in vivo* than cultured cell lines. We also employed longer IPG strips (24 cm) for a better separation of total proteins. Furthermore, in order to improve the accuracy of the differentially expressed protein profile, merely protein spots exhibiting expression differences with a high degree of statistical confidence ($P < 0.01$) were selected for mass spectrometry analysis, though some protein spots may have been omitted. Finally, 54 unique differentially expressed proteins were identified in SOC versus normal ovarian epithelium. To the best of our awareness, 16 of 54 proteins were reported here for the first time to be dysregulated in cancerous tissues, 24 of 54 proteins have been previously reported as dysregulated in the other types of cancer, whereas additional 14 proteins have been previously reported to be dysregulated in ovarian carcinoma at protein or gene level. Six proteins were selected for further analysis, including BANF1, galectin-1, GGCT, GMFB, HDGF and Rho GDI 2.

Table 3 – Univariate and multivariate analyses for disease-free and overall survival rates of individual parameters.

	Disease-free survival			Overall survival		
	HR	95% CI	P	HR	95% CI	P
Univariate						
Age	0.919	0.569–1.484	0.729	1.388	0.793–2.429	0.250
FIGO stage‡	2.552	1.630–3.998	<0.001**	2.760	1.601–4.757	<0.001**
Tumour grade	1.075	0.631–1.831	0.789	0.930	0.509–1.700	0.814
Clinical response to chemotherapy	0.293	0.180–0.478	<0.001**	0.229	0.130–0.403	<0.001**
Performance status	1.379	0.837–2.273	0.207	1.452	0.815–2.585	0.206
Pretreatment serum CA125	1.600	0.965–2.652	0.068	1.521	0.855–2.704	0.154
Ascitic fluid volume	2.142	1.204–3.812	0.010*	2.819	1.370–5.802	0.005**
Residual disease	1.982	1.219–3.222	0.006**	1.980	1.141–3.436	0.015*
GMFB expression†	2.279	1.219–4.260	0.010*	3.536	1.540–8.119	0.003**
Multivariate						
Age	0.973	0.568–1.669	0.922	1.148	0.598–2.203	0.679
FIGO stage‡	1.936	1.094–3.426	0.023*	2.487	1.163–5.316	0.019*
Tumour grade	1.043	0.575–1.893	0.889	0.767	0.384–1.531	0.451
Clinical response to chemotherapy	0.431	0.241–0.772	0.005**	0.308	0.160–0.594	<0.001**
Performance status	1.191	0.656–2.163	0.565	1.552	0.800–3.013	0.194
Pretreatment serum CA125	0.931	0.489–1.774	0.828	0.974	0.483–1.966	0.942
Ascitic fluid volume	1.262	0.612–2.601	0.529	1.531	0.654–3.587	0.327
Residual disease	1.240	0.690–2.229	0.472	1.235	0.633–2.411	0.535
GMFB expression†	2.075	1.092–3.942	0.026*	3.417	1.431–8.162	0.006**

Abbreviation: HR, hazard ratio; 95% CI, 95% confidence interval.

* Significant at the 0.05 level.

** Significant at the 0.01 level.

† Low + moderate versus high.

‡ I versus II versus III versus IV.

Western blot analysis of the six proteins validated that the differential expressions of proteins obtained from proteomic analysis were convincing.

The expression levels of the six genes corresponding above-mentioned six proteins were also evaluated by real-time RT-PCR. Combining proteomic and transcriptional analyses of the same set of samples may help to understand the complicated mechanisms influencing protein expression in SOC. *BANF1*, *LAGLS1*, *HDGF* and *ARHGDIB* mRNA alterations were coherent with the protein changes. However, *GGCT* and *GMFB* mRNA expression showed no difference in normal and cancerous groups, suggesting that the expressions of the two proteins are likely to be influenced by translation and post-translational mechanisms in these tissues.

GGCT, GMFB, HDGF and Rho GDI 2 are all upregulated proteins and have not been studied in relation to ovarian cancer. In western blot analysis, compared to normal tissues they exhibited more than 6-fold, 9-fold, 4-fold and 2-fold overexpression, respectively. Moreover, they also occurred with high frequency in SOC patients (90–100%).Thus, our findings suggest that these four proteins may be promising candidate tumour markers for SOC.

GMFB was first found and purified by Lim and colleagues[24] as a brain protein. It was originally identified as a growth and differentiation factor for neurons as well as glia.[25,26] Later, Zaheer and colleagues[27] found that overexpressed GMFB in neuroblastoma N18 cells by gene infection induced caspase-dependent apoptosis mediated by GSK-3β activation. It has recently been reported that GMFB also plays as an intracellular regulator of stress-activated signal transduction.[28–30] In addition to the nervous system, GMFB expression was also found in the thymus and intestine.[31,32] We reported here for the first time that GMFB was expressed in normal ovarian epithelium and cancerous tissues outside the nervous system. More importantly, we found a significantly increased expression of GMFB in SOC tissues by proteomics and Western blot. We further investigated alterations of GMFB expression in various ovarian epithelial lesions in a larger sample set (a total of 246 cases) by immunohistochemical analysis. Consequently, we evaluated the association of GMFB expression with clinicopathological features of SOC and survival of the patients. We found that GMFB expression in SOC was significantly increased than that in normal epithelium, benign serous adenoma and borderline serous adenoma tissues, thus we confirmed the results of proteomics and western blot in a large clinical sample. GMFB could seem to help distinguish the SOC from benign and borderline adenomas. Moreover, we also found that increased GMFB staining was associated with advanced FIGO stage of SOC. In order to further understand the clinical significance of GMFB, we analysed the correlation between its expression and survival of SOC patients. We found that patients with high GMFB expression exhibited lower disease-free and overall survival rates. In a subsequently more detailed survival study, univariate and multivariate analyses revealed that GMFB is an independent prognostic factor for both disease-free and overall survival. Our findings suggested that GMFB may be involved in the progression of SOC and it can probably be employed as a predictor for patient prognosis and survival in SOC. The results imply that a further investigation on whether GMFB can be used as a therapeutic target for SOC is warranted.

GGCT, previously known as CRF21 and hypothetical protein c7orf24, is recently demonstrated to be an essential enzyme in the gamma-glutamyl cycle.[33] It has been implicated with a potential role in the induction of apoptosis by the release of cytochrome c from mitochondria.[34] But in a subsequent study, it was found to be related to tumour cell proliferation in bladder cancer.[35] However, there has been no report demonstrating an association between GGCT expression and ovarian cancer as yet. In the present study, we noted obvious overexpression of GGCT in SOC by both proteomics and western blot analysis. However, the detailed biological roles of GGCT in SOC remain to be further elucidated.

HDGF is a heparin-binding growth factor, and considered to be closely related to the ontogeny and aggressive biological potential of cancer cells.[36–40] Accumulating findings demonstrate that HDGF is a prognosticator of various tumours such as hepatocellular, gastric and pancreatic cancers.[41–45] Surprisingly, there has no published report about HDGF expression in gynaecological cancers. Here, we found that HDGF was upregulated in SOC compared with normal ovarian epithelium. Based on its role as a growth factor and previous findings in other cancers, it is possible that increased expression of HDGF may promote tumour cell proliferation and contribute to tumour progression in SOC.

Another protein observed to be upregulated in SOC was Rho GDI 2, an inhibitor of Rho GTPases widely expressed in hematopoietic cells. Rho family GTPase are involved in a number of processes related to tumour metastasis. Rho GDIs regulate Rho family proteins. Previous studies have shown that Rho GDI 2 functions in colon cancer metastasis by anchoring Rho proteins to the cell membrane.[46] Moreover, it has been found that Rho GDI 2 is overexpressed in breast cancer cell lines and promotes its invasiveness.[47] However, in bladder and lung cancer, Rho GDI 2 suppresses invitation and metastasis.[48,49] Schunke and colleagues have demonstrated that Rho GDI 2 has two opposing activities: one that suppresses tumour progression by inhibiting migration and other that stimulates tumour progression by enhancing tumour promoter protein Cox-2 expression.[50] Whether Rho GDI 2 is merely a potential expression marker or it also contributes to tumour metastasis and progression in SOC remains to be determined.

BANF1 was also found to be significantly downregulated in SOC tissues in our study. BANF1 is a DNA-binding protein identified to protect retroviruses from intramolecular integration and therefore promotes intermolecular integration into the host cell genome. Haraguchi and colleagues[51] demonstrated that BANF1 performed an important function in cell cycle progression and nuclear organisation. It is the fist time to detect BANF1 protein expression in cancerous tissues. We conjecture that decreased BANF1 expression in SOC may cause disorder of cellular cycle control and abnormal proliferation of ovarian cancer cells. However, the definite effect of the deficiency of BANF1 expression in SOC requires further investigation.

Galectin-1 is a member of a carbohydrate-binding protein family with an affinity for β-galactosides. Interestingly, as Choufani and colleagues[52] have found, Galectins are frequently overexpressed in cancerous cells and cancer-associated stromal cells, especially in those cell types that do not normally express the specific galectins, such as pancreatic,[53,54] colorectal[55] cancer cells and melanoma cells.[56] Controversially, when normal cells do express high levels of selected galectins, these galectins are downregulated when those cells become cancerous, such as head and neck cancer cells.[57] In our study, Galectin-1 was highly expressed in both normal and SOC tissues, and relatively downregulated in SOC, which is well consistent with the findings mentioned above. It has been thought that altered galectin expression is related to the aggressiveness of tumour and the acquisition of the metastatic phenotype.[52] Thus, our findings suggested that downregulation of galectin-1 is probably associated with SOC development. In conclusion, our findings suggest that the six proteins we identified here may be involved in the development or progression of SOC, and GMFB can be considered as a predictor for prognosis of SOC patients.

Conflict of interest statement

None declared.

Acknowledgement

We appreciate financial support from the National Natural Science Foundation of China (No. 30672230, No. 30672229 and No. 30973380).

Appendix A. Supplementary material

Supplementary data associated with this article can be found, in the online version, at doi:10.1016/j.ejca.2010.04.015.

REFERENCES

1. Parkin DM, Bray F, Ferlay J, Pisani P. Global cancer statistics, 2002. *CA Cancer J Clin* 2005;**55**:74–108.
2. Jemal A, Murray T, Samuels A, et al. Cancer statistics, 2003. *CA Cancer J Clin* 2003;**3**:5–26.
3. Fehrmann RS, Li XY, van der Zee AG, et al. Profiling studies in ovarian cancer: a review. *Oncologist* 2007;**12**:960–6.
4. Konstantinopoulos PA, Spentzos D, Cannistra SA. Gene-expression profiling in epithelial ovarian cancer. *Nat Clin Pract Oncol* 2008;**5**:577–87.
5. Chen G, Gharib TG, Huang CC, et al. Discordant protein and mRNA expression in lung adenocarcinomas. *Mol Cell Proteomics* 2002;**1**:304–13.
6. Anderson L, Seilhamer J. A comparison of selected mRNA and protein abundances in human liver. *Electrophoresis* 1997;**18**:533–7.
7. Gygi SP, Rochon Y, Franza BR, Aebersold R. Correlation between protein and mRNA abundance in yeast. *Mol Cell Biol* 1999;**19**:1720–30.
8. Köbel M, KallogerSE BoydN, McKinney S, et al. *PLoS Med* 2008;**5**:e232.
9. An HJ, Kim DS, Park YK, et al. Comparative proteomics of ovarian epithelial tumors. *J Proteome Res* 2006;**5**:1082–90.
10. Bengtsson S, Krogh M, Szigyarto CA, et al. Large-scale proteomics analysis of human ovarian cancer for biomarkers. *J Proteome Res* 2007;**6**:1440–50.

11. Bradford MM. A rapid and sensitive method for the quantitation of microgram quantities of protein utilizing the principle of protein–dye binding. *Anal Biochem* 1976;**72**:248–54.
12. Yan JX, Wait R, Berkelman T, et al. A modified silver staining protocol for visualization of proteins compatible with matrix-assisted laser desorption/ionization and electrospray ionization–mass spectrometry. *Electrophoresis* 2000;**21**:3666–72.
13. Gharahdaghi F, Weinberg CR, Meagher DA, Imai BS, Mische SM. Mass spectrometric identification of proteins from silver-stained polyacrylamide gel: a method for the removal of silver ions to enhance sensitivity. *Electrophoresis* 1999;**20**:601–5.
14. Sarbia M, Loberg C, Wolter M, et al. Expression of bcl-2 and amplification of c-myc are frequent in basaloid squamous cell carcinomas of the esophagus. *Am J Pathol* 1999;**155**:1027–32.
15. Hao XP, Pretlow TG, Rao JS, Pretlow TP. Bata-catenin expression is altered in human colonic aberrant crypt foci. *Cancer Res* 2001;**61**:8085–8.
16. Zhang L, Ding F, Cao W, et al. Stromatin-like protein 2 is overexpressed in cancer and involved in regulating cell growth and cell adhesion in human esophageal squamous cell carcinoma. *Clin Cancer Res* 2006;**12**:1639–46.
17. Gabriel B, zur Hausen A, Stickeler E, et al. Weak expression of focal adhesion kinase (pp125FAK) in patients with cervical cancer is associated with poor disease outcome. *Clin Cancer Res* 2006;**12**:2476–83.
18. Gagné JP, Gagné P, Hunter JM, et al. Proteome profiling of human epithelial ovarian cancer cell line TOV-112D. *Mol Cell Biochem* 2005;**275**:25–55.
19. Gagné JP, Ethier C, Gagné P, et al. *Proteome Sci* 2007;**5**:16.
20. Morita A, Miyagi E, Yasumitsu H, et al. Proteomic search for potential diagnostic markers and therapeutic targets for ovarian clear cell adenocarcinoma. *Proteomics* 2006;**6**:5880–90.
21. Ismail RS, Baldwin RL, Fang J, et al. Differential gene expression between normal and tumor derived ovarian epithelial cells. *Cancer Res* 2000;**60**:6744–9.
22. Tonin PN, Hudsno TJ, Rodier F, et al. Microarray analysis of gene expression mirrors the biology of ovarian cancer model. *Oncogene* 2001;**20**:6617–26.
23. Li XQ, Zhang SL, Cai Z, et al. Proteomic identification of tumor-associated protein in ovarian serous cystadenocarinoma. *Cancer Lett* 2009;**275**:109–16.
24. Lim R, Mitsunobu K. Brain cells in culture: morphological transformation by a protein. *Science* 1974;**185**:63–6.
25. Kaplan R, Zaheer A, Jaye M, Lim R. Molecular cloning and expression of biologically active human glia maturation factor beta. *J Neurochem* 1991;**57**:483–90.
26. Nishiwaki A, Asai K, Tada T, et al. Expression of glia maturation factor during retinal development in the rat. *Brain Res Mol Brain Res* 2000;**95**:103–9.
27. Zaheer A, Knight S, Zaheer A, et al. Glia maturation factor overexpression in neuroblastoma cells activates glycogen synthase kinase-3β and caspase-3. *Brain Res* 2008;**1190**:206–14.
28. Zaheer A, Lim R. In vitro inhibition of MAP kinase (ERK1/ERK2) activity by phosphorylated glia maturation factor (GMF). *Biochemistry* 1996;**35**:6283–8.
29. Zaheer A, Lim R. Protein kinase A (PKA)- and protein kinase C-phosphorylated glia maturation factor promotes the catalytic activity of PKA. *J Biol Chem* 1997;**272**:5183–6.
30. Zaheer A, Lim R. Overexpression of glia maturation factor (GMF) in PC12 pheochromocytoma cells activates p38 MAP kinase, MAPKAP kinase-2, and tyrosine hydroxylase. *Biochem Biophys Res Commun* 1998;**250**:228–78.
31. Zaheer A, Yorek MA, Lim R. Effects of glia maturation factor overexpression in primary astrocytes on MAP kinase activation, transcription factor activation, and neurotrophin secretion. *Neurochem Res* 2001;**6**:1293–9.
32. Utsuyama M, Shiraishi J, Takahashi H, Kasai M, Hirokawa K. Glia maturation factor produced by thymic epithelial cells plays a role in T cell differentiation in the thymic microenvironment. *Int Immunol* 2003;**15**:557–64.
33. Oakley AJ, Yamada T, Liu D, et al. The identification and structural characterization of C7orf24 as gamma-glutamyl cyclotransferase. An essential enzyme in the gamma-glutamyl cycle. *J Biol Chem* 2008;**283**:2031–42.
34. Masuda Y, Maeda S, Watanabe A, et al. A novel 21-kDa cytochrome c-releasing factor is generated upon treatment of human leukemia U937 cells with geranylgeraniol. *Biochem Biophys Res Commun* 2006;**346**:454–60.
35. Kageyama S, Iwaki H, Inoue H, et al. A novel tumor-related protein, C7orf24, identified by proteome differential display of bladder urothelial carcinoma. *Proteomics Clin Appl* 2007;**1**:192–9.
36. Everett AD, Lobe DR, Matsumura ME, Nakamura H, McNamara CA. Hepatoma-derived growth factor stimulates smooth muscle cell growth and is expressed in vascular development. *J Clin Invest* 2000;**105**:567–75.
37. Enomoto H, Yoshida K, Kishima Y, et al. Hepatoma-derived growth factor is highly expressed in developing liver and promotes fetal hepatocyte proliferation. *Hepatology* 2002;**36**:1519–27.
38. Lepourcelet M, Tou L, Cai L, et al. Insights into developmental mechanisms and cancers in the mammalian intestine derived from serial analysis of gene expression and study of the hepatoma-derived growth factor (HDGF). *Development* 2005;**132**:415–27.
39. Kishima Y, Yoshida K, Enomoto H, et al. Antisense oligonucleotides of hepatoma-derived growth factor (HDGF) suppress the proliferation of hepatoma cells. *Hepatogastroenterology* 2002;**49**:1639–44.
40. Okuda Y, Nakamura H, Yoshida K, et al. Hepatoma-derived growth factor induces tumorigenesis in vivo through both direct angiogenic activity and induction of vascular endothelial growth factor. *Cancer Sci* 2003;**94**:1034–41.
41. Uyama H, Tomita Y, Nakamura H, et al. Hepatoma-derived growth factor is a novel prognostic factor for patients with pancreatic cancer. *Clin Cancer Res* 2006;**12**:6043–8.
42. Hu TH, Lin JW, Chen HH, et al. The expression and prognostic role of hepatoma-derived growth factor in colorectal stromal tumors. *Dis Colon Rectum* 2009;**52**:319–36.
43. Chang KC, Tai MH, Lin JW, et al. Hepatoma-derived growth factor is a novel prognostic factor for gastrointestinal stromal tumors. *Int J Cancer* 2007;**121**:1059–65.
44. Yoshida K, Tomita Y, Okuda Y, et al. Hepatoma-derived growth factor is a novel prognostic factor for hepatocellular carcinoma. *Ann Surg Oncol* 2006;**13**:159–67.
45. Yamamoto S, Tomita Y, Hoshida Y, et al. Expression of hepatoma-derived growth factor is correlated with lymph node metastasis and prognosis of gastric carcinoma. *Clin Cancer Res* 2006;**12**:117–22.
46. Ota T, Maeda M, Suto S, Tatsuka M. LyGDI functions in cancer metastasis by anchoring Rho proteins to the cell membrane. *Mol Carcinogen* 2004;**39**:206–20.
47. Zhang Y, Zhang B. D4-GDI, a Rho GTPase regulator, promotes breast cancer cell invasiveness. *Cancer Res* 2006;**66**:5592–8.
48. Gildea JJ, Seraj MJ, Oxford G, et al. RhoGDI2 is an invasion and metastasis suppressor gene in human cancer. *Cancer Res* 2002;**62**:6418–23.
49. Titus B, HFJr Frierson, Conaway M, et al. Endothelin axis is a target of the lung metastasis suppressor gene RhoGDI2. *Cancer Res* 2005;**65**:7320–7.
50. Schunke D, Span P, Ronneburg H, et al. Cyclooxygenase-2 is a target gene of rho GDP dissociation inhibitor beta in breast cancer cells. *Cancer Res* 2007;**67**:694–702.

51. Haraguchi T, Koujin T, Osakada H, et al. Nuclear localization of barrier-to-autointegration factor is correlated with progression of S phase in human cells. *J Cell Sci* 2007;**20**:67–77.
52. Choufani G, Nagy N, Saussez S, et al. The levels of expression of galectin-1, galectin-3, and the Thomsen–Friedenreich antigen and their binding sites decrease as clinical aggressiveness increases in head and neck cancers. *Cancer* 1999;**86**:2353–63.
53. Shen J, Person MD, Zhu J, Abbruzzese JL, Li D. Protein expression profiles in pancreatic adenocarcinoma compared with normal pancreatic tissue and tissue affected by pancreatitis as detected by two-dimensional gel electrophoresis and mass spectrometry. *Cancer Res* 2004;**64**:9018–26.
54. Pan S, Chen R, Reimel BA, et al. Quantitative proteomics investigation of pancreatic intraepithelial neoplasia. *Electrophoresis* 2009;**30**:1132–44.
55. Watanabe M, Takemasa I, Kawaguchi N, et al. An application of the 2-nitrobenzenesulfenyl (NBS) method to proteomic profiling of human colorectal carcinoma: a novel approach for biomarker discovery. *Proteomics Clin Appl* 2008;**2**:925–35.
56. Rubinstein N, Alvarez M, Zwirner NW, et al. Targeted inhibition of galectin-1 gene expression in tumor cells results in heightened T cell-mediated rejection: a potential mechanism of tumor-immune privilege. *Cancer Cell* 2004;**5**:241–51.
57. Plzák J, Betka J, Smetana Jr K, et al. Galectin-3 – an emerging prognostic indicator in advanced head and neck carcinoma. *Eur J Cancer* 2004;**40**:2324–30.